Available online at www.sciencedirect.com

SciVerse ScienceDirect

Ceramics International 39 (2013) 5615–5621

CERAMICS INTERNATIONAL

www.elsevier.com/locate/ceramint

Luminescence improvement of $Y_2O_2S:Tb^{3+}$, Sr^{2+}, Zr^{4+} white-light long-lasting phosphor via Eu^{3+} addition

Ping Huang[a], Fan Yang[a], Cai'e Cui[a,b,*], Lei Wang[a], Xing Lei[a]

[a]*Physics and Optoelectronic Engineering College, Taiyuan University of Technology, Taiyuan 030024, China*
[b]*Observation and Control Technology Research Institute, Taiyuan University of Technology, Taiyuan 030024, China*

Received 12 November 2012; received in revised form 18 December 2012; accepted 23 December 2012
Available online 5 January 2013

Abstract

In order to improve the luminescence properties of $Y_2O_2S:Tb^{3+}$, Sr^{2+}, Zr^{4+}, the Eu^{3+} ions doped $Y_2O_2S:Tb^{3+}$, Sr^{2+}, Zr^{4+} white-light long-lasting phosphors were synthesized by the solid-state reaction method. The $Y_2O_2S:Tb^{3+}$, Eu^{3+}, Sr^{2+}, Zr^{4+} phosphors were characterized by X-ray diffraction, photoluminescence, long-lasting phosphorescence and thermoluminescence spectra. The samples doped with different concentration of Eu^{3+} ions were composed of the pure Y_2O_2S phase at 1000 °C for 30 min. Under 263 nm UV excitation, the emission peaks at 417 nm and 544 nm were assigned to the $^5D_3 \rightarrow {}^7F_5$ and $^5D_4 \rightarrow {}^7F_5$ transitions of Tb^{3+} respectively, and the emission peak at 626 nm was assigned to the $^5D_0 \rightarrow {}^7F_2$ transition of Eu^{3+}. With 0.15% Eu^{3+} concentration, the CIE chromaticity diagram was (0.28, 0.31), the trap depth was 0.89 eV and the decay time could last for over 220 s (≥ 1 mcd/m^2).

Keywords: White-light long-lasting phosphors; Yttrium oxysulfide; Rare earths

1. Introduction

Long-lasting phosphors are a special kind of photoluminescent materials, which can still light up for a long time after removal of the excitation source. They are widely used in several fields such as emergency lighting, road signs, safety indication, and decorative craft. So far, the colors of developed long-lasting phosphors cover most of the region from blue to red [1–5]. However, the white-light long-lasting phosphors are still under investigation because the afterglow decay process of the different color emissions which are mixed to produce white emission is not consistent, and the luminescence properties of the white-light long-lasting phosphors cannot meet the application requirements. In those published literatures, the white-light long-lasting phosphors mainly include rare-earth Dy^{3+}-doped silicates [6–8] and aluminates [9], and rare-earth Tb^{3+}-doped yttrium oxysulfides [10–11]. In all these materials, the white long-lasting emission is got via the combination of different color emissions from an identical luminescence center in the same host. Among them, $Y_2O_2S:Tb^{3+}$ phosphor is a good material for the development of long-lasting phosphor due to the stable chemical and physical properties of Y_2O_2S host and the high luminescence efficiency of Tb^{3+} ion. For $Y_2O_2S:Tb^{3+}$ phosphor, the white-light is obtained by the appropriate mixing of the blue emission at 417 nm and the green emission at 544 nm. However, the color of phosphor is far from the ideal white because the red emission of Tb^{3+} ion is very weak. A very natural idea is suggested to improve the white-light emission by co-doping the red emitting ion into $Y_2O_2S:Tb^{3+}$ phosphor. In those reported literatures, $Y_2O_2S:Eu^{3+}$, Mg^{2+}, Ti^{4+} phosphor is an excellent red long-lasting phosphor [3], and the red emission at 626 nm is assigned to the transition of Eu^{3+}. So, it is possible that the ideal white-light long-lasting can be achieved by synchronously doping Tb^{3+} and Eu^{3+} ions into the Y_2O_2S host.

In this paper, white-light long-lasting phosphors $Y_2O_2S:Tb^{3+}$, Eu^{3+}, Sr^{2+}, Zr^{4+} are prepared through the solid state reaction method and the effects of Eu^{3+} content on the crystal characteristics, luminescent properties and afterglow performance of $Y_2O_2S:Tb^{3+}$, Eu^{3+}, Sr^{2+}, Zr^{4+} phosphors are discussed.

*Corresponding author at: Physics and Optoelectronic Engineering College, Taiyuan University of Technology, Taiyuan 030024, China. Tel.: +86 351 4175345.
E-mail address: tytgcejy@sina.com (C. Cui).

0272-8842/$ - see front matter © 2013 Elsevier Ltd and Techna Group S.r.l. All rights reserved.
http://dx.doi.org/10.1016/j.ceramint.2012.12.077

2. Experimental

The powder samples with a stoichiometric ratio of Y_2O_2S: 0.3% Tb^{3+}, 0.05–0.2% Eu^{3+}, 4% Sr^{2+}, 4% Zr^{4+} were prepared by the solid-state reaction. Y_2O_3 (3N), Tb_4O_7 (4N), Eu_2O_3 (4N), $SrCO_3$ (AR), ZrO_2 (AR), S (CP) were used as raw materials, Na_2CO_3 (AR) and $K_3PO_4 \cdot 3H_2O$ (AR) were added as flux. The molar ratio of Y_2O_3: S: Na_2CO_3: $K_3PO_4 \cdot 3H_2O$ component was 1: 1.98: 0.67: 0.1. The raw materials and flux were thoroughly mixed and ground. The mixtures were calcined from 950 °C to 1200 °C for 30 min in reduced atmosphere with subsequent air cooling to get the products.

X-ray powder diffraction (XRD) was performed to check the phase of the samples at 40 kV and 30 mA using a SHIMADZU-6000 X-ray generator with Cu Kα ($\lambda = 0.15406$ nm) radiation and the scan step was 0.02°. Excitation and emission spectra of the powder samples were measured using an F-280 fluorescence spectrophotometer with a 150 W Xe lamp as excitation source. The afterglow intensity decay curves of different emissions were measured using an F-7000 fluorescence spectrophotometer. The excitation light was switched off after the sample had been excited with 263 nm UV for 1 min. The afterglow decay curves were measured by the brightness meter (ST-86LA). Thermoluminescence (TL) spectra of samples were measured on a model FJ-427A1TL meter with a heating rate of 1 K/s from room temperature to 673 K. The samples were excited for 10 min by 254 nm UV radiation standard lamp with a power of 6 W before measuring their TL curves and the afterglow decay curves. All the measurements were performed at room temperature except for the TL spectra.

3. Results and discussion

3.1. Phase characterization

Fig. 1 indicate power X-ray diffraction (XRD) patterns of Y_2O_2S:Tb^{3+}, Sr^{2+}, Zr^{4+} phosphors calcined at different temperatures. After heating the mixture of raw materials at 950 °C for 30 min, the powder becomes a mixture of cubic Y_2O_3 crystalline phase and hexagonal Y_2O_2S crystalline phase, in which Y_2O_3 is a major phase. At 1000 °C and 1050 °C, the diffraction peaks of Y_2O_3 disappear, and pure Y_2O_2S phase is formed. The intensity of the Y_2O_2S diffraction peaks increases with the increase of the calcination temperature, which indicates that the crystallinity of the Y_2O_2S increases more perfectly with the increase of the calcination temperature. In Fig. 1, the crystallization of the Y_2O_2S entirely forms at 1000 °C. Above 1050 °C, the diffraction peak positions and shapes of powders are similar to that of those calcined at 950 °C. But the intensity of the diffraction peak (101) of Y_2O_2S is decreased gradually owing to the decomposition of Y_2O_2S with the increase of calcination temperature. So, the optimal calcination temperature for the sample is 1000 °C to produce

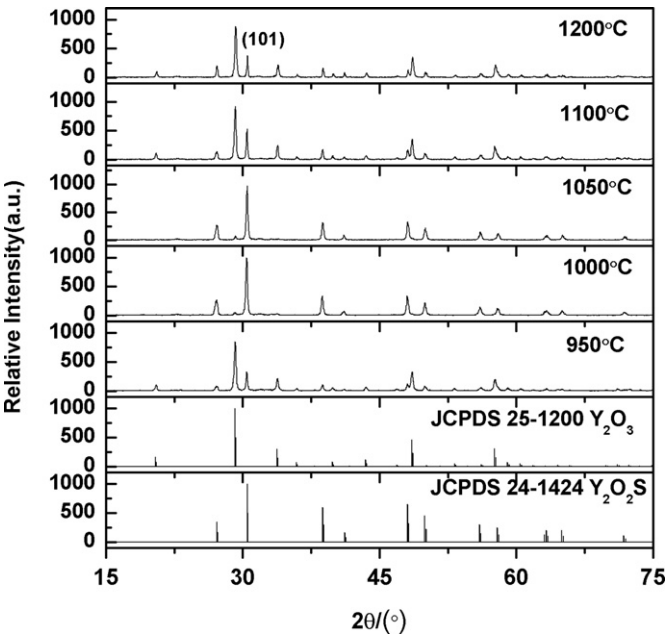

Fig. 1. The XRD patterns of Y_2O_2S: Tb^{3+}, Sr^{2+}, Zr^{4+} phosphor obtained at different temperatures and JCPDS Cards no. 25-1200, no. 24-1424.

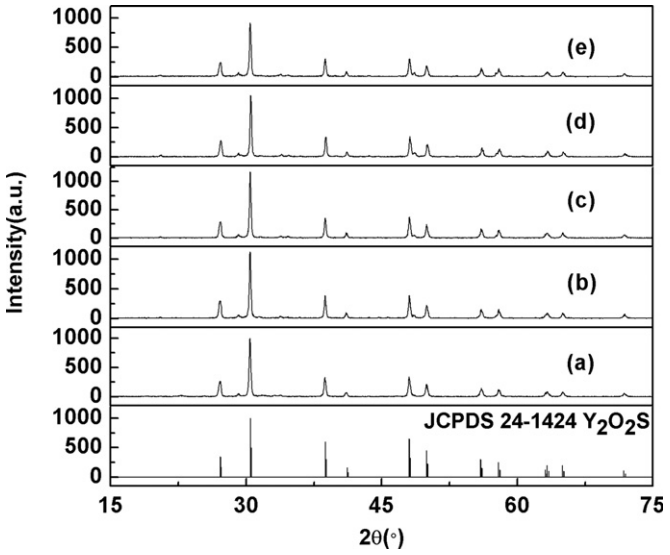

Fig. 2. The XRD patterns of Y_2O_2S:Tb^{3+}, Eu^{3+}, Sr^{2+}, Zr^{4+} phosphor with different concentrations of Eu^{3+} (a) 0%; (b) 0.05%; (c) 0.10%; (d) 0.15%; (e) 0.20% and JCPDS Card no. 24-1424.

pure Y_2O_2S phase. The samples with different concentration of Eu^{3+} will also be obtained at this temperature. There is no other evident phase observed in XRD patterns of samples excepting Y_2O_3 and Y_2O_2S. It illustrates that co-doping a certain amount of Tb^{3+}, Sr^{2+} and Zr^{4+} does not influence the basic crystal structure.

Fig. 2 indicate power X-ray diffraction (XRD) patterns of Y_2O_2S: Tb^{3+}, Eu^{3+}, Sr^{2+}, Zr^{4+} phosphors calcined at 1000 °C with different concentration of Eu^{3+}. All the samples are composed by pure Y_2O_2S phase which accords

with the JCPDS Card no. 24-1424. There is no other evident phase observed in XRD patterns of samples excepting Y_2O_2S. It illustrates that co-doping a certain amount of Eu^{3+} does not influence the basic crystal structure.

3.2. Luminescent spectra and CIE chromaticity diagram of samples

By monitoring the 544 nm and 626 nm emissions from the Tb^{3+} and Eu^{3+} ions respectively, the excitation spectra of Y_2O_2S: Tb^{3+}, 0.15% Eu^{3+}, Sr^{2+}, Zr^{4+} phosphor are shown in Fig. 3. For the curve A, the peak about 263 nm is attributed to the absorption band of Y_2O_2S host lattice [12], and the broad band peak near 288 nm corresponds to 4f→5d transition of Tb^{3+} ion [13]. For the curve B, the peaks at 263 nm and 325 nm are assigned to the Eu^{3+}–S^{2-} CTB (charge transfer band) and Eu^{3+}–O^{2-} CTB respectively, and the peaks about 397 nm and 469 nm correspond to f→f transitions of Eu^{3+} [14]. The excitation spectra of the other samples are similar to Fig. 3. So they are not shown here.

The emission spectra of samples with different concentration of Eu^{3+} are shown in Fig. 4. It is composed of the transitions from $^5D_3 \rightarrow {}^7F_J$ and $^5D_4 \rightarrow {}^7F_J$ (J=0, 1, 2…6) of Tb^{3+}[10], and the transitions from ^5D_J (J=0,1,2)→^7F_J (J=0,1,2,3,4) of Eu^{3+} [15]. The emission peaks at 417 nm (blue light) and 544 nm (green light) are assigned to the $^5D_3 \rightarrow {}^7F_5$ and $^5D_4 \rightarrow {}^7F_5$ transitions of Tb^{3+} respectively, and the peak at 626 nm (red light) is assigned to the $^5D_0 \rightarrow {}^7F_2$ transition of Eu^{3+}. The white-light can be obtained by the appropriate mixing of them. With the increase of Eu^{3+} content, the intensity of emission peaks of Tb^{3+} is decreased gradually, which indicates that there is energy transfer from Tb^{3+} to Eu^{3+} ions [16]. At the same time, the intensity of emission peaks of Eu^{3+} is increased initially and then decreased. The value reaches a maximum when Eu^{3+} content is 0.15%. The reason may be that the self-quenching of Eu^{3+} operates. On the one hand, there is energy transfer from Tb^{3+} to Eu^{3+}, which leads to an increase of the Eu^{3+} emission. But on the other hand, self-quenching of Eu^{3+} mechanism causes an increase in extent of non-radiative transitions, which leads to a decrease of the Eu^{3+} emission. The self-quenching of Eu^{3+} mechanism predominates over the energy transfer from Tb^{3+} to Eu^{3+} process for sample containing high concentration of Eu^{3+} ions and this is responsible for the decrease in the intensity of emission peaks of Eu^{3+}. In addition, when Eu^{3+} concentration is high, the number of near-neighbor Tb^{3+} ions will be less and this reduces the extent of energy transfer between Tb^{3+} and Eu^{3+} ions [17].

The CIE chromaticity diagram of Y_2O_2S:Tb^{3+}, Eu^{3+}, Sr^{2+}, Zr^{4+} phosphors with different concentration of Eu^{3+} is shown in Fig. 5. The CIE chromaticity coordinates of samples can be obtained by the emission spectra. They vary systematically from (0.20, 0.26), (0.23, 0.28), (0.26, 0.29), (0.28, 0.31) to (0.27, 0.28), corresponding to point A, B, C, D and E. With the increase of Eu^{3+} content, the proportion of red and green emissions from Eu^{3+} is increased and meanwhile the blue emission from Tb^{3+} is decreased. As a result, the chromaticity coordinates values increase. When Eu^{3+} concentration increases to 0.15%, self-quenching of Eu^{3+} operates, and then the emissions of Eu^{3+} decrease, which leads to the decrease of the chromaticity coordinates values. This change is consistent with Fig. 4. In Fig. 5, point D is the closest to point W (0.33, 0.33) which delegates the ideal white. This indicates that the sample doped with 0.15% Eu^{3+} is the most suitable for white-light generation.

The afterglow intensity decay curves of the 417 nm, 544 nm and 626 nm emissions in Y_2O_2S:Tb^{3+}, 0.15% Eu^{3+}, Sr^{2+}, Zr^{4+} phosphor after irradiation with 263 nm UV radiation for 1 min are shown in Fig. 6. The decay curves of the 417 nm, 544 nm and 626 nm emissions are similar. This indicates that the emissions have similar decay ratio. Thereby, a stable white emission in the sample can be produced during the decay process.

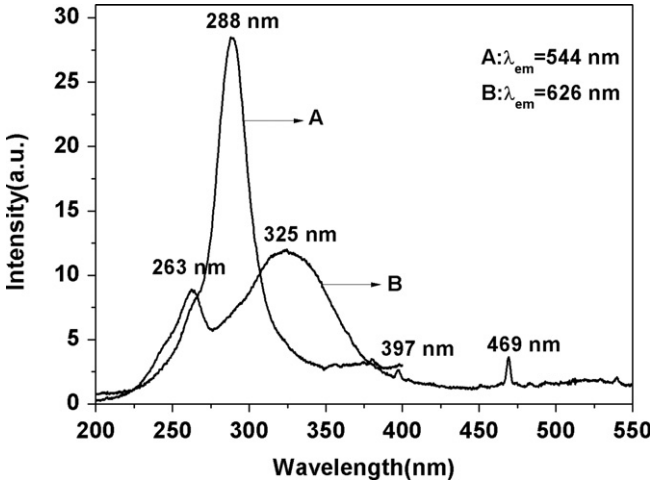

Fig. 3. The excitation spectra of Y_2O_2S: Tb^{3+}, 0.15% Eu^{3+}, Sr^{2+}, Zr^{4+} phosphor.

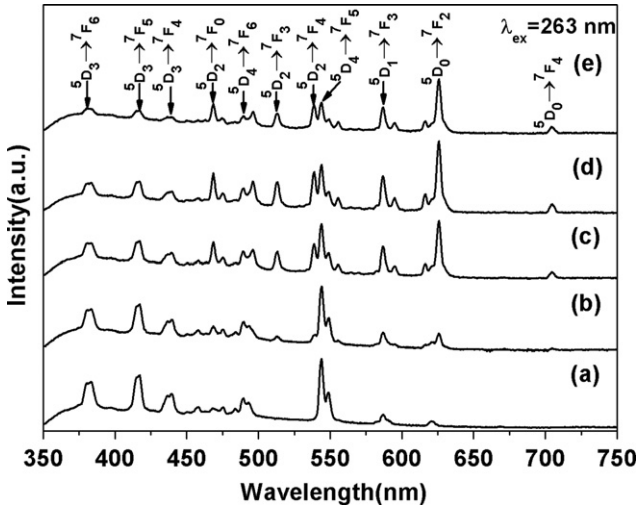

Fig. 4. The emission spectra of Y_2O_2S: Tb^{3+}, Eu^{3+}, Sr^{2+}, Zr^{4+} phosphor with different concentrations of Eu^{3+} (a) 0%; (b) 0.05%; (c) 0.10%; (d) 0.15%; (e) 0.20%.

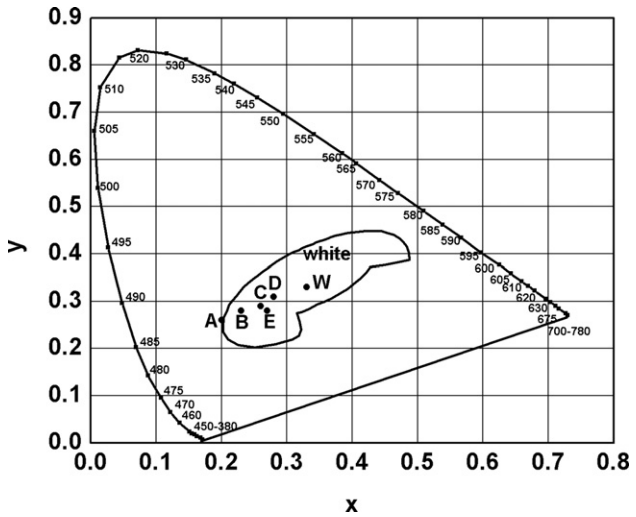

Fig. 5. The CIE chromaticity diagram of Y_2O_2S: Tb^{3+}, Eu^{3+}, Sr^{2+}, Zr^{4+} phosphor with different concentration of Eu^{3+} (a) 0%; (b) 0.05%; (c) 0.10%; (d) 0.15%; (e) 0.20%.

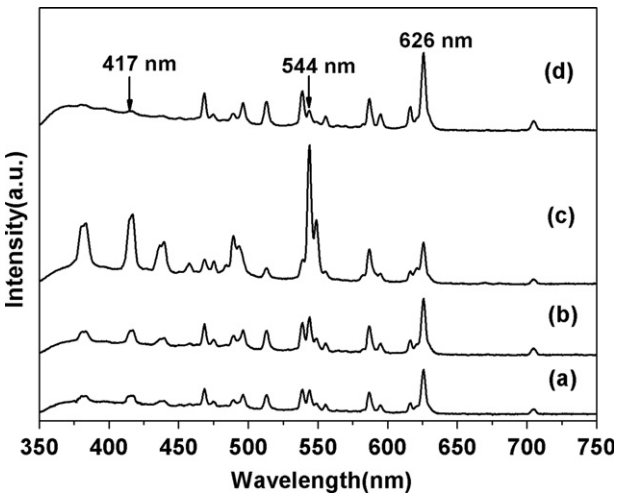

Fig. 7. The emission spectra of Y_2O_2S: Tb^{3+}, 0.15% Eu^{3+}, Sr^{2+}, Zr^{4+} phosphor excited with different wavelengths (a) 254 nm; (b) 263 nm; (c) 288 nm; (d) 325 nm.

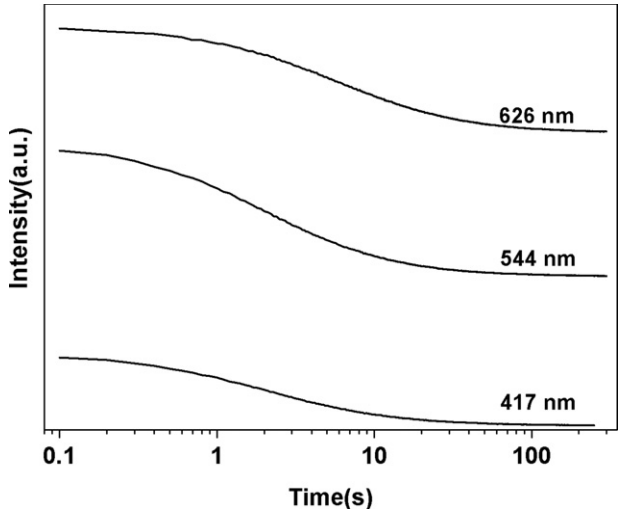

Fig. 6. Afterglow intensity decay curves of different emissions in Y_2O_2S: Tb^{3+}, 0.15% Eu^{3+}, Sr^{2+}, Zr^{4+} phosphor.

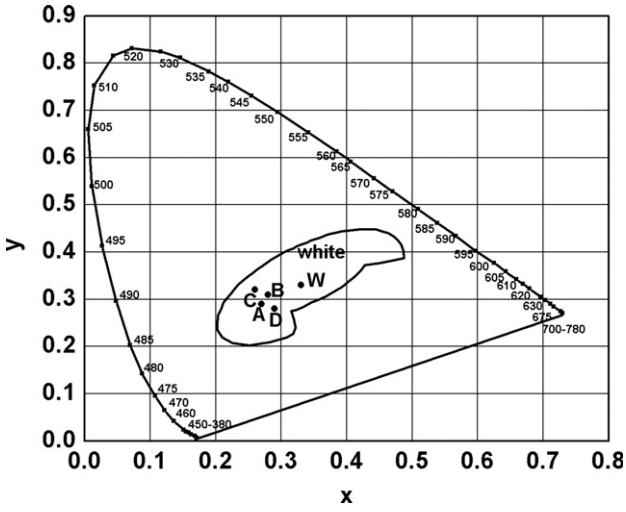

Fig. 8. The CIE chromaticity diagram of Y_2O_2S: Tb^{3+}, 0.15% Eu^{3+}, Sr^{2+}, Zr^{4+} phosphor excited with different wavelengths A 254 nm; B 263 nm; C 288 nm; D 325 nm.

The emission spectra of Y_2O_2S:Tb^{3+}, 0.15% Eu^{3+}, Sr^{2+}, Zr^{4+} phosphor excited with different wavelengths are shown in Fig. 7. The sample mainly shows a strong 626 nm (red) emission from Eu^{3+} when it is excited by 325 nm wavelength, and the sample primarily shows strong 417 nm (blue) and 544 nm (green) emissions from Tb^{3+} when it is excited by 288 nm wavelength. The blue, green and red emissions can be simultaneously excited by 254 nm or 263 nm UV light, but the latter is stronger than the former. The emission intensity can be adjusted by changing the excitation wavelength. This is also consistent with Fig. 3.

The CIE chromaticity diagram of Y_2O_2S:Tb^{3+}, 0.15% Eu^{3+}, Sr^{2+}, Zr^{4+} phosphor excited with different wavelengths is shown in Fig. 8. The CIE chromaticity coordinates of (0.27, 0.29), (0.28, 0.31), (0.26, 0.32) and (0.29, 0.28) correspond to point A, B, C and D respectively, and point B is the closest to point W (0.33, 0.33). This suggests that the luminescence color can be adjusted by varying the excitation wavelength. In order to simultaneously excite the Tb^{3+} and Eu^{3+} ions to get white-light emission, 263 nm UV light appears to be the appropriate excitation wavelength.

3.3. Afterglow decay curves and TL curves of samples

The afterglow decay curves of samples undoped and doped with 0.15% Eu^{3+} after irradiation with 254 nm UV radiation for 10 min are shown in Fig. 9. The decay curves are fitted by initial rapid decay and then a stable decay. Compared with the sample undoped Eu^{3+}, the afterglow

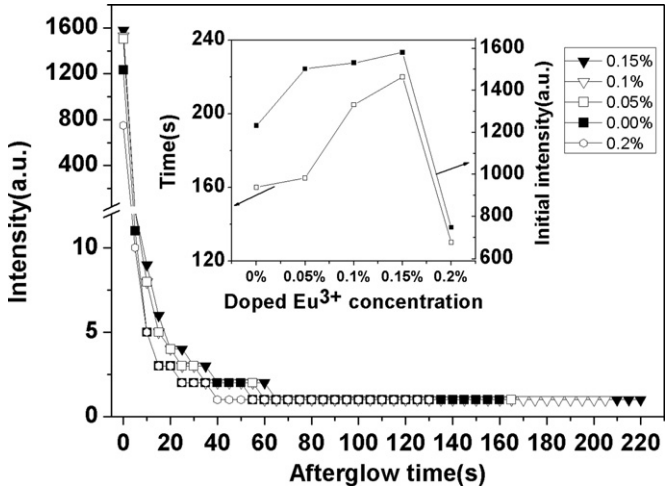

Fig. 9. The afterglow decay curves of Y_2O_2S: Tb^{3+}, Eu^{3+}, Sr^{2+}, Zr^{4+} phosphor (the inset picture shows the initial intensity and afterglow time with different concentration of Eu^{3+}).

Table 1
Fitting parameters of samples.

Concentration of Eu^{3+}-doped (mol)	Parameters	
	τ_1	τ_2
0	1.20399	0.09058
0.15%	1.23598	0.12135

properties of sample doped with 0.15% Eu^{3+} is slightly improved. The sample doped with 0.15% Eu^{3+} shows the optimal initial luminance and afterglow time, which are 1581 mcd/m^2 and 220 s ($\geq$1 mcd/m^2) respectively. It is reported that the decay behavior of long lasting phosphors can be calculated by fitting the decay data using the following equation [18]:

$$I = I_0 + A_1\exp(-t/\tau_1) + A_2\exp(-t/\tau_2) \quad (1)$$

where I and I_0 are the phosphorescence intensities; A_1 and A_2 are constants; t is time; τ_1 and τ_2 are the decay times for the exponential components, respectively. Using the software of Origin 8.0, the parameters of both the samples with and without the addition Eu^{3+} ions can be obtained, which are listed in Table 1. The values of τ_1 are bigger than τ_2, which implies that the decay processes of phosphors are fitted by initial rapid decay and then a stable decay. Meanwhile, the values of the decay times of the sample doped with 0.15% Eu^{3+} are all bigger than that sample undoped Eu^{3+}, which illustrates that by doping Eu^{3+}, the sample shows a better afterglow property. The afterglow mechanisms can be explained by the contribution from the electron traps formed by the co-doped Sr^{2+} and Zr^{4+} ions. They occupy the same lattice sites as Y^{3+} ions do. To keep charge balance, 2 Y^{3+} ions are replaced by 1 Sr^{2+} and 1 Zr^{4+} ion. However, such replacement breaks the charge balance around local lattice site and causes the formation of new electronic donating and accepting levels between the host lattice band gap, that is, an excessive positive charge which serves as the electron trap around the doped Zr^{4+} ion is created. One of the ions absorbs energy and thermally transfers the excited electrons to another ion which serves as trap centers. The trap of stored energy which is constituted by Sr^{2+} and Zr^{4+} ions serves as the donor leveling, and Tb^{3+} and Eu^{3+} ions serve as the acceptor leveling. The trapping of excited electrons and thermally released processes cause the appearance of afterglow [15].

TL spectrum is an important tool to investigate the luminous properties of phosphor. The afterglow luminance and time are found to depend strongly on the depth and the density of traps [19,20]. Fig. 10 represents the TL curves of samples with different concentration of Eu^{3+} after irradiation with 254 nm UV radiation for 10 min. For all the samples, the TL peaks are located in the region of 323–383 K which are helpful to produce a longer duration of afterglow [21]. In Fig. 10(a), the TL peak is located in the 358 K. From the report [15], the TL peak is around 360 K. Both of them are so close, which implies that the trap type of Y_2O_2S host doped Tb^{3+} is similar to that of it doped Eu^{3+}. So, only one TL peak can be observed in each sample. With the increase of content of Eu^{3+} ions, the intensity of TL peak is increased gradually, and the intensity of TL peak reaches maximum when the concentration of Eu^{3+} ions is 0.15%, implying that the co-doped Eu^{3+} ions can improve the trap density. When

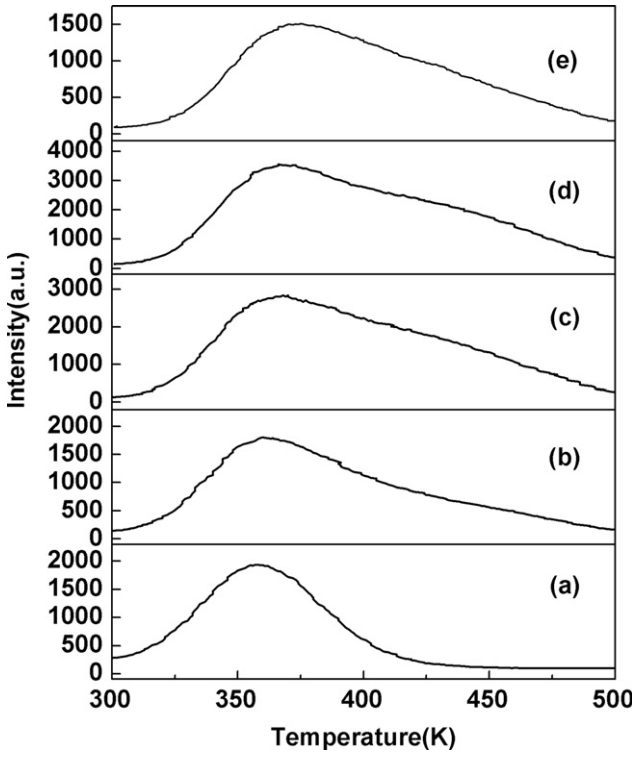

Fig. 10. The TL curves of Y_2O_2S: Tb^{3+}, Eu^{3+}, Sr^{2+}, Zr^{4+} phosphor with different concentrations of Eu^{3+} (a) 0%; (b) 0.05%; (c) 0.10%; (d) 0.15%; (e) 0.20%.

Table 2
E values of the samples with different concentration of Eu^{3+}.

Concentration of Eu^{3+}-doped (%)	T_m/K	T_1/K	T_2/K	τ/K	δ/K	ω/K	μ_g	E/eV
0.00	358	331	390	27	32	59	0.54	0.64
0.05	360	333	414	27	54	81	0.67	0.77
0.10	370	337	444	33	74	107	0.69	0.66
0.15	366	339	449	27	83	110	0.75	0.89
0.20	375	343	444	32	69	101	0.68	0.70

the concentration of Eu^{3+} ions exceeds 0.15%, the intensity of TL peak begins to decrease because concentration quenching of Eu^{3+} ions occurs [22].

The depth of traps in samples can be estimated by analyzing the TL peak using equations given by Chen [23].

$$E = c_\tau k T_m^2/\tau - b_\tau 2kT_m \quad (2)$$

$$c_\tau = 1.51 + 3(\mu_g - 0.42),\ b_\tau = 1.58 + 4.2(\mu_g - 0.42) \quad (3)$$

$$\tau = T_m - T_1,\ \delta = T_2 - T_m,\ \omega = T_2 - T_1,\ \mu_g = \delta/\omega \quad (4)$$

where T_m is the peak temperature, T_1 and T_2 are the low and high temperatures corresponding to the half peak intensity, τ is the left half width, δ is the right half width, ω is the total half intensity width, k is the Boltzmann's constant, μ_g is the symmetry factor. The trap parameters are calculated using Eqs. (2)–(4) and listed in Table 2.

In order to produce long phosphorescence, the trapping levels need to locate at a suitable depth. If the trap level is too shallow, only small amount of electrons can be captured to traps. Under the action of thermal disturbances, electrons are easily released from traps and then combined with holes in the ground state, which results in shorter afterglow time. On the other hand, if the trap level is too deep, the electrons are hard to return to the excited state levels at room temperature, which also results in poor afterglow property. In Table 2, compared with the sample undoped, the trap depth of samples can be improved by doping Eu^{3+}. The sample doped with 0.15% Eu^{3+} has the deepest trap depth with 0.89 eV, and it shows the optimal initial luminance and afterglow time. From Fig. 10 and Table 2, for the Y_2O_2S:Tb^{3+}, Eu^{3+}, Sr^{2+}, Zr^{4+} phosphor, the high trap density and deep trap depth is suitable to produce optimal afterglow properties.

4. Conclusions

The white-light long-lasting phosphors Y_2O_2S:Tb^{3+}, Eu^{3+}, Sr^{2+}, Zr^{4+} with different concentration of Eu^{3+} are prepared through the solid state reaction method. Pure Y_2O_2S phase can be obtained at 1000 °C for 30 min in reduced atmosphere. Under the 263 nm UV irradiation, the white-light can be obtained by the appropriate mixing of the blue emission at 417 nm and green emission at 544 nm of Tb^{3+}, and red emission at 626 nm of Eu^{3+}. The sample doped with 0.15% Eu^{3+} has the highest trap density and the deepest trap depth, which leads to the optimal initial luminance and afterglow time. Therefore, for the white-light long-lasting phosphor, the optimal concentration of Eu^{3+} is 0.15%.

Acknowledgments

This present work was financially supported by the National Natural Science Foundation of China (No. 51072128), the Key Research Project of Science and Technology of Shanxi (No. 2011 0321040-01) and the Program for the Top Young Academic Leaders of Higher Learning Institutions of Shanxi.

References

[1] T. Matsuzawa, Y. Aoki, N. Takeuchi, Y. Murayama, A new long phosphorescent phosphor with high brightness $SrAl_2O_4$:Eu^{2+}, Dy^{3+}, Journal of the Electrochemical Society 143 (1996) 2670–2673.
[2] S.Y. Kaya, E. Karacaoglu, B. Karasu, Effect of Al/Sr ratio on the luminescence properties of $SrAl_2O_4$:Eu^{2+}, Dy^{3+} phosphors, Ceramics International 38 (2012) 3701–3706.
[3] Y. Murazaki, K. Arak, K. Ichinomiya, A new long persistence red phosphor, Journal of Rare Earths Japan 35 (1999) 41–45.
[4] H.H. Zeng, X.M. Zhou, L. Zhang, X.P. Dong, Synthesis and luminescence properties of a novel red long lasting phosphor Y_2O_2S: Eu^{3+}, Si^{4+}, Zn^{2+}, Journal of Alloys and Compounds 460 (2008) 704–707.
[5] W. Pan, G.L. Ning, X. Zhang, J. Wang, Y. Lin, J.W. Ye, Enhanced luminescent properties of long-persistent $Sr_2MgSi_2O_7$:Eu^{2+}, Dy^{3+} phosphor prepared by the co-precipitation method, Journal of Luminescence 128 (2008) 1975–1979.
[6] Y.L. Liu, B.F. Lei, C.S. Shi, Luminescent properties of a white afterglow phosphor $CdSiO_3$:Dy^{3+}, Chemistry of Materials 17 (2005) 2108–2113.
[7] J.Y. Kuang, Y.L. Liu, J.X. Zhang, White-light-emitting long-lasting phosphorescence in Dy^{3+}-doped $SrSiO_3$, Journal of Solid State Chemistry 179 (2006) 266–269.
[8] Y.H. Chen, X.R. Cheng, Z.M. Qi, M. Liu, C.S. Shi, Comparison study of the luminescent properties of the white-long afterglow phosphors:$Ca_xMgSi_2O_{5+x}$:Dy^{3+}(x=1,2,3), Journal of Luminescence 129 (2009) 531–535.
[9] B. Liu, C.S. Shi, Z.M. Qi, Potential white-light long-lasting phosphor Dy^{3+}-doped aluminate, Applied Physics Letters 86 (2005) 191111.
[10] B. Liu, C.S. Shi, Z.M. Qi, White-light long-lasting phosphorescence from Tb^{3+}-activated Y_2O_2S phosphor, Journal of Physics and Chemistry of Solids 67 (2006) 1674–1677.
[11] L. Lin, K. Chen, Z.F. Wang, B.G. You, Y.H. Chen, W.P. Zhang, C.S. Shi, A white long lasting phosphor Y_2O_2S:Tb^{3+},Sm^{3+}:an improvement of Y_2O_2S:Tb^3, Journal of Rare Earths 26 (2008) 648–651.
[12] Z.L. Wang, Y.H. Wang, J.C. Zhang, Y.H. Lu, The photoluminescence properties of Eu^{3+},Bi^{3+}co-doped yttrium oxysulfide phosphor under vacuum ultraviolet excitation, Materials Research Bulletin 44 (2009) 1183–1187.

[13] S.A. Xia, T. Chen, C.K. Duan, Interpretation of the 4f–5d excitation spectra of Eu^{3+} and Tb^{3+} doped in crystals, Journal of Rare Earths 24 (2006) 400–407.

[14] S.Q. Deng, Z.P. Xie, Y.L. Liu, B.F. Lei, Y. Xiao, M.T. Zheng, Synthesis and characterization of $Y_2O_2S:Eu^{3+}$, Mg^{2+}, Ti^{4+} hollow nanospheresvia a template-free route, Journal of Alloys and Compounds 542 (2012) 207–212.

[15] P.F. Ai, W.Y. Li, L.Y. Xiao, Y.D. Li, H.J. Wang, Y.L. Liu, Monodisperse nanospheres of yttrium oxysulfide: synthesis, characterization, and luminescent properties, Ceramics International 36 (2010) 2169–2174.

[16] Z. Liu, L.X. Yu, Q. Wang, Y.C. Tao, H. Yang, Effect of Eu, Tb codoping on the luminescent properties of Y_2O_3 nanorods, Journal of Luminescence 131 (2011) 12–16.

[17] S. Mukherjee, V. Sudarsan, R.K. Vatsa, S.V. Godbole, R.M. Kadam, U.M. Bhatta, A.K. Tyagi, Effect of structure, particle size and relative concentration of Eu^{3+} and Tb^{3+} ions on the luminescence properties of Eu^{3+} co-doped Y_2O_3:Tb, Nanotechnology 19 (2008) 325704.

[18] B.F. Lei, B. Li, H.R. Zhang, W.L. Li, Preparation and luminescence properties of $CaSnO_3:Sm^{3+}$ phosphor emitting in the reddish orange region, Optical Materials 29 (2007) 1491–1494.

[19] T. Aitasalo, P. Dereń, J. Hölsä, H. Jungner, J.C. Krupa, M. Lastusaari, J. Legendziewicz, J. Niittykoski, W. Stręk, Persistent luminescence phenomena in materials doped with rare earth ions, Journal of Solid State Chemistry 171 (2003) 114–122.

[20] L. Jing, C.K. Chang, D.L. Mao, B. Zhang, A new long persistent blue-emitting $Sr_2ZnSi_2O_7:Eu^{2+}$, Dy^{3+} prepared by sol-gel method, Materials Letters 58 (2004) 1825–1829.

[21] P.F. Ai, Y.L. Liu, L.Y. Xiao, H.J. Wang, J.X. Meng, Synthesis of $Y_2O_2S:Eu^{3+}$, Mg^{2+}, Ti^{4+} hollow microspheres via homogeneous precipitation route, Science and Technology of Advanced Materials 11 (2010) 035002 (5pp).

[22] S.W.S. Mckeever, Thermoluminescence of Solids, Cambridge University Press, New York, 1988, pp. 150–151.

[23] R. Chen, Glow curves with general order kinetics, Journal of Electrochemical Society: Solid State Science 116 (1969) 1254–1257.